The Impact of Near-Ground Path Loss Modeling on Wireless Sensor Network Lifetime

Huseyin Ugur Yildiz*, Sinan Kurt†, and Bulent Tavli*

*TOBB University of Economics and Technology, Ankara, Turkey, E-mail: {huyildiz, btavli}@etu.edu.tr
†ASELSAN Inc., Ankara, Turkey, E-mail: sinank@aselsan.com.tr

***Abstract*—Network lifetime is the ultimate objective in evaluating the performance of Wireless Sensor Networks (WSNs). To assess the network lifetime correctly for a particular WSN deployment, utilizing realistic abstractions for modeling various aspects of system components are crucial. The overwhelming majority of the studies on the WSN lifetime maximization utilize well known theoretical path loss models like the two-ray model, however, such models do not lead to realistic path loss results. In this study, we formulate a detailed link level model of WSNs utilizing Mica2 motes and, based on the link layer model, we construct a novel Mixed Integer Program (MIP) to analyze the effects of path loss models on the WSN lifetime. By exploring the parameter space through numerical evaluations of the MIP model, we characterize the impact of path loss models on the WSN lifetime.**

***Index Terms*—wireless sensor networks, network lifetime, energy efficiency, path loss models, mixed integer programming.**

I. Introduction

The maximization of network lifetime, arguably, is the most important performance metric for Wireless Sensor Networks (WSNs), which can be achieved by optimizing the energy dissipation of the network as a whole. Communication and computation are the two fundamental classes for energy dissipation of sensor nodes. However, the generally accepted view on WSNs is that communication energy dissipation is the dominant term which is supported by the results obtained from actual WSN testbed experiments [1]. Therefore, the optimization of energy dissipation for communication is vital for WSN lifetime maximization.

In practical WSN platforms (*e.g.*, Mica2 and TelosB), there are finite levels of transmission power levels. Depending on the path loss value between the transmitter and the receiver, optimal power level that achieves the target Bit Error Rate (BER), should be used to avoid unnecessary energy dissipation. In WSN literature, most of the studies on lifetime optimization utilize certain theoretical models (*e.g.*, free-space, two-ray) as path loss models due to the simplicity of these models [2], [3]. However, experimental studies on path loss modeling for WSNs [4], [5], reveal that aforementioned theoretical models produce significant path loss estimation errors, especially for the cases where antennas are placed near-ground (*e.g.*, antenna heights are less than a wavelength). If the path loss model(s) used for node pairs do not reflect the actual path losses to be experienced in the network, then the network lifetime computed based on the path loss model(s) may fail to accurately predict the actual network lifetime, hence, it is imperative to employ accurate models of path loss in a network for accurately predicting the network lifetime.

Although comparative evaluations of various path loss models for WSNs are performed in the literature [4]–[6], the impact of path loss modeling on the WSN lifetime has not been investigated. Indeed, the differences between path loss values given by different models show significant variations, however, how do these differences project on the network lifetime is yet to be investigated. Hence, in this study we fill the gap in the literature by performing comparative analysis on the effects of path loss models on the WSN lifetime. We developed a novel Mixed Integer Program (MIP) for WSN lifetime maximization by incorporating the major energy dissipation mechanisms of Mica2 motes and characterized the parameter space by numerical evaluations of the MIP model.

II. Path Loss Models

Propagation models focus, mainly, on predicting the average signal strength drop at different transmitter receiver separations. These models can be pure theoretical or measurement based. If possible, using a measurement based model suitable for the scenario under consideration is the best choice. Unfortunately, measurement based models are not always readily available. Therefore, it is desirable to assess the level of accuracy that can be achieved by employing a particular theoretical path loss model for the WSN scenario under consideration. In the following subsections we, succinctly, summarize the prominent path loss models used in WSN research.

A. Free-Space Model

Free-space propagation model can be used when there are no obstacles in the line-of-sight (LOS) path from transmitter to receiver and LOS path is the dominating one. The model is based on Friis transmission equation in which spherical propagation is considered and can be expressed as

$$P_r = \frac{P_t G_t G_r \lambda^2}{(4\pi)^2 d^2}, \tag{1}$$

where P_t is transmitter power, G_t is the transmitter antenna gain, G_r is receiver antenna gain, λ is wavelength, and d is transmitter receiver distance. For most practical cases the assumptions of the free-space model do not hold (*i.e.*, there

may be other paths besides the LOS path or there may not be a LOS path, at all).

B. Two-Ray (Ground Reflection) Model

Considering terrestrial applications, when the transmitter and the receiver antennas are not very close to the ground two-ray model comes up with a useful formulation based on geometric optics by incorporating both the direct path and the ground reflected waves. To calculate power at the receiver, vector sum of LOS E-field, and reflected E-field are used. Two-ray model is heavily utilized, especially in theoretical studies, for a wide range of application domains. However, generally, it is used by making many assumptions and simplifications that come with it. For large values of d, simplified version of the received power (P_r) becomes [7]

$$P_r = P_t G_t G_r \frac{h_t^2 h_r^2}{d^4}. \tag{2}$$

where h_t and h_r are defined as the heights of the transmitting and receiving antennas, respectively. Although two-ray model is an elegant theoretical model, it is important to check whether the assumptions come with it are applicable to the scenario under consideration, especially when the antennas are on or near the ground. Also note that reflection coefficient of the ground, which is assumed to be 1 for large d values, changes with polarization of the waves. The reflection coefficients for polarizations parallel (*i.e.*, vertical polarization) to ($\Gamma_\parallel$) and perpendicular (*i.e.*, horizontal polarization) to ($\Gamma_\perp$) the plane of incidence can be expressed as

$$\Gamma_\parallel = \frac{-\varepsilon_r sin\theta_i + \sqrt{\varepsilon_r - cos\theta_i^2}}{\varepsilon_r sin\theta_i + \sqrt{\varepsilon_r - cos\theta_i^2}}, \tag{3}$$

$$\Gamma_\perp = \frac{sin\theta_i - \sqrt{\varepsilon_r - cos\theta_i^2}}{sin\theta_i + \sqrt{\varepsilon_r - cos\theta_i^2}}, \tag{4}$$

where ε_r is relative permittivity of ground which is taken as 15 throughout this work [7]. Since incorporation of the reflection coefficients into two-ray model without simplifying assumptions are quite involved we refer the interested readers to reference [7].

C. Log-Normal Shadowing

It is an experimental fact that there are random variations in path loss due to environmental clutter, object blockage in propagation path, or from changes in reflecting and scattering objects (*e.g.*, relative movement). As a result, path loss for different locations having the same transmitter receiver distances can differ considerably. Non-deterministic characteristics of path loss can be captured by using statistical models. The most common model for characterization of non-deterministic effects in wireless path loss modeling is log-normal shadowing. A zero mean Gaussian distributed random variable with standard deviation σ is used to abstract the deviations from the deterministic path loss mechanism (*i.e.*, exponential decay with an exponent of n). In practical applications n and σ values are computed by using linear regression of measured data.

1) One-Slope Log-Normal Model: One-slope log-normal model is based on log-normal shadowing model and can be expressed as

$$PL(d) = PL(d_0) + 10n \log(\frac{d}{d_0}) + X_\sigma, \tag{5}$$

where $PL(d)$ is in dB and $PL(d_0)$ is the path loss at a reference distance (d_0) in the proximity of the transmitter. d_0 is usually taken as 1 m, 100 m or 1 km according to application ranges of the model. $PL(d_0)$ is sometimes set to free-space path loss at d_0 or alternatively it can be determined by measurements at d_0. In [4], [5], one-slope log-normal models for WSNs are obtained by curve fitting the path loss data obtained from field measurements.

2) Two-Slope Log-Normal Model: In one-slope log-normal model, it is assumed that the path loss can be expressed by a single path loss exponent value and a single shadowing standard deviation value, however, experimental studies on WSN path loss estimation [4] reveal that utilization of a two-slope log-normal model results in a better representation of the measured data. Two-slope log-normal path loss model can, mathematically, be expressed as follows

$$PL(d) = \begin{cases} PL(d_{01}) + 10n_1 \log(d) + X_{\sigma 1} & \text{if } d \leq d_b \\ PL(d_{02}) + 10n_2 \log(d) + X_{\sigma 2} & \text{if } d > d_b \end{cases}, \tag{6}$$

where model given in (5) is used with different slope regions separated at a breakpoint distance d_b.

There are several other path loss models developed specifically for terrestrial WSNs [6], however, aforementioned models are the prominent models.

III. System Model

In this section, we give an overview of the system model and present the link layer model that will form the foundations for the MIP model elaborated in Section IV.

A. Overview

The network consists of a stationary base station and a plurality of stationary sensor nodes which are roughly time synchronized. We assume that the base station has the complete topology information (*e.g.*, path losses on each link) and sufficiently high processing and energy resources to perform the necessary computation for data flow planning in a centralized manner. A TDMA-based MAC layer is in operation which mitigates interference between active links through a time-slot assignment algorithm. In fact, in our model, we use the sufficient condition presented in [8] which outputs a conflict-free transmission schedule. Path loss for each link is measured by a closed loop power control mechanism.

All data generated at sensor nodes terminate at the base station (*i.e.*, convergecast traffic) either directly (single-hop) or through other sensor nodes acting as relays (multi-hop). In addition, generated data packets at sensor nodes are treated as atomic data units that cannot be fragmented or aggregated at any relay node. Time is organized into constant duration

rounds ($T_{rnd} = 20$ s). At each round each sensor node generates s_i number of data packets. Data exchange between node pairs are accomplished via a two-way handshake mechanism (data packets are replied with ACK packets). Each sensor node can select transmission power level from a finite set for both data and ACK packets. The objective of our problem is to maximize the network lifetime that is the duration between the time network starts operating and the time when the first sensor node in the network exhausts all its energy [3], [9]. To maximize the lifetime, all the nodes are forced to dissipate their energies in a balanced fashion (*i.e.*, their battery energies are depleted almost simultaneously).

B. Data Link Layer Model

We utilize Mica2 motes' energy consumption characteristics equipped with CC1000 radios which are the most heavily utilized sensor nodes in experimental WSN research due to their well-characterized energy dissipation properties [10]. In Table I, power consumption of the transceiver and the corresponding output antenna power for Mica2 motes are presented. In this table, $P_{tx}^{crc}(l)$ and $P_{tx}^{ant}(l)$ refer to the power consumption for transmission at power level-l, and the output antenna power at power level-l, respectively. The set of power levels is denoted as S_L. Power consumption for reception is constant and taken as 35.4 mW ($P_{rx}^{crc} = 35.4$ mW).

At each round energy dissipation for data acquisition is $E_{DA} = 600$ μJ. The size of a data packet is taken as 100 Bytes (*i.e.*, $M_P = 100$ Bytes). The size of an ACK packet is $M_A = 20$ Bytes. The slot time (T_{slot}) is taken as 51 ms. The received signal power ($P_{rx,ij}^{ant}(l)$) due to a transmission at power level-l over the link-(i,j) is

$$P_{rx,ij}^{ant}(l)[\text{dBm}] = P_{tx}^{ant}(l)[\text{dBm}] - \Upsilon_{ij}[\text{dB}], \tag{7}$$

where Υ_{ij} denotes the calculated path loss value over link (i,j) (see Section V for the parameters of the path loss models presented in Section II). Signal-to-noise ratio (SNR) is

$$\psi_{ij}(l)[\text{dB}] = P_{rx,ij}^{ant}(l)[\text{dBm}] - P_n[\text{dBm}], \tag{8}$$

where the noise power (P_n) is -115 dBm at the temperature of 300 Kelvin for Mica2 motes [11]. The probability of a successful packet reception [11] of a φ-Byte packet transmitted at power level-l over the link-(i,j) is

$$p_{ij}^{s}(l,\varphi) = \left(1 - \frac{1}{2}\exp\left(\frac{-\psi_{ij}(l)}{2}\frac{1}{0.64}\right)\right)^{8\varphi}, \tag{9}$$

and the failure probability is calculated as

$$p_{ij}^{f}(l,\varphi) = 1 - p_{ij}^{s}(l,\varphi). \tag{10}$$

The probability of a successful handshake when the data packet is transmitted at power level-l and acknowledged at power level-k over the link-(i,j) is

$$p_{ij}^{HS,s}(l,k) = p_{ij}^{s}(l,M_P) \times p_{ji}^{s}(k,M_A), \tag{11}$$

provided that $P_{rx,ij}^{ant}(l) \geq P_{sns}$ and $P_{rx,ji}^{ant}(k) \geq P_{sns}$. Otherwise (*i.e.*, $P_{rx,ij}^{ant}(l) < P_{sns}$ or $P_{rx,ji}^{ant}(k) < P_{sns}$), $p_{ij}^{HS,s}(l,k) = 0$ where P_{sns} denotes the reception sensitivity of the Mica2 motes (P_{sns} = -102 dBm) [10]. The probability of a failed handshake is given as

$$p_{ij}^{HS,f}(l,k) = 1 - p_{ij}^{HS,s}(l,k). \tag{12}$$

On the average, each data packet has to be transmitted $\lambda_{ij}(l,k) = 1/p_{ij}^{HS,s}(l,k)$ times. Energy dissipation for transmitting M_P Bytes of data from node-i to node-j at power level-l is

$$E_{tx}^{P}(l,M_P) = P_{tx}^{crc}(l)T_{tx}(M_P), \tag{13}$$

where $T_{tx}(M_P)$ is the duration of a data packet which is obtained by dividing the number of bits by the channel data rate ($\xi = 19.2$ Kbps) [12]. Likewise, $T_{tx}(M_A)$ denotes the duration of an ACK packet. A node stays in receiving mode when it is not transmitting. Hence, the total energy dissipation of a transmitter in a slot (during a single handshake) is

$$E_{tx}^{HS}(l,M_P) = E_{tx}^{P}(l,M_P) + P_{rx}^{crc}(T_{slot} - T_{tx}(M_P)). \tag{14}$$

Transmitter's energy dissipation including packet failures and processing cost ($E_{PP} = 120$ μJ) is

$$E_{tx,ij}^{D}(l,k) = E_{PP} + \lambda_{ij}(l,k)E_{tx}^{HS}(l,M_P). \tag{15}$$

Energy dissipation for receiving a data packet and replying with an ACK packet without any packet error (*i.e.*, successful handshake) is

$$E_{rx}^{HS,s}(k,M_A) = P_{rx}^{crc}(T_{slot} - T_{tx}(M_A)) + E_{tx}^{P}(k,M_A). \tag{16}$$

If the handshake failure caused by the bit errors in the received data packet then the energy cost for reception can be expressed as

$$E_{rx}^{HS,f} = P_{rx}^{crc}T_{slot}. \tag{17}$$

Receiver's energy dissipation including the effects of packet failures can be obtained as

$$E_{rx,ji}^{D}(l,k) = E_{rx}^{HS,s}(k,M_A) + E_{PP} + \lambda_{ij}(l,k) \left[p_{ij}^{s}(l,M_P)p_{ji}^{f}(k,M_A)E_{rx}^{HS,s}(k,M_A) + p_{ij}^{f}(l,M_P)E_{rx}^{HS,f}\right] \tag{18}$$

TABLE I: Transmission power consumption ($P_{tx}^{crc}(l)$ in mW) and output antenna power ($P_{tx}^{ant}(l)$ in mW) at each power level (l) for the Mica2 motes equipped with CC1000 [10].

l	$P_{tx}^{crc}(l)$	$P_{tx}^{ant}(l)$	l	$P_{tx}^{crc}(l)$	$P_{tx}^{ant}(l)$
1	25.8	0.0100	14	32.4	0.1995
2	26.4	0.0126	15	33.3	0.2512
3	27.0	0.0158	16	41.4	0.3162
4	27.1	0.0200	17	43.5	0.3981
5	27.3	0.0251	18	43.6	0.5012
6	27.8	0.0316	19	45.3	0.6310
7	27.9	0.0398	20	47.4	0.7943
8	28.5	0.0501	21	50.4	1.0000
9	29.1	0.0631	22	51.6	1.2589
10	29.7	0.0794	23	55.5	1.5849
11	30.3	0.1000	24	57.6	1.9953
12	31.2	0.1259	25	63.9	2.5119
13	31.8	0.1585	26	76.2	3.1623

IV. MIP Framework

In this section, we present the MIP framework used to model our power control strategy for various path loss models to maximize WSN lifetime. The network topology is represented by a directed graph, $G = (V, A)$, where V denotes the set of all nodes including the base station as node-1. We also define set W which includes all nodes except node-1 (*i.e.*, $W = V \backslash \{1\}$). $A = \{(i, j) : i \in W, j \in V - i\}$ is the ordered set of arcs. Note that the definition of A implies that no node sends data to itself. The amount of data (*i.e.*, the number of data packets) flowing from node-i to node-j is represented as f_{ij}.

The optimization problem is presented in Figure 1. Note that unitless variable N_{rnd} gives the network lifetime in terms of number of rounds and the actual network lifetime can be expressed by the product $N_{rnd} \times T_{rnd}$.

Equation (20) is the flow balancing constraint at each sensor node (*i.e.*, $\forall i \in W$). It states that data flowing into node-i plus data generated by node-i is equal to the data flowing out of node-i. Equation (21) ensures that all data generated at each source node eventually flows into the base station (node-1). Total busy time in a sensor node is obtained as in Equation (22). Equation (23) is the energy balancing constraint which states that for all nodes except the base station total energy dissipation is bounded by the energy stored in batteries (ϱ). Energy dissipation terms on the left side of inequality in this equation accounts for transmission, sleep, reception, and data acquisition energies, respectively. Note that if a node is neither a receiver nor a transmitter at any slot or if it is not acquiring data then it is in the sleep mode. Power consumption in sleep mode is taken as 30 μW (*i.e.*, $P_{slp} = 30$ μW). Each sensor node is provided equal initial energy ($\varrho = 10$ KJ) at the beginning of the network operation. The constraint for bandwidth is presented in Equation (24). In this equation it is guaranteed that the channel bandwidth required to perform communication operations at each node is strictly bounded by the available bandwidth. For all nodes including the base station the aggregate duration of incoming flows, outgoing flows, and interfering flows is upper bounded by the total network lifetime. This constraint is a modified version of the sufficient condition given in [8]. We refer to the flows around node-i which are not flowing into or flowing out of node-i, however, affect the available bandwidth of node-i as interfering flows. Interference function ($I^i_{jn}(l, k)$) is formulated in Equation (25). If node-i is in the interference region of the transmission from node-j to node-n at power level-l (data transmission) or node-n to node-j at power level-k (ACK transmission), then the value of interference function for node-i is unity ($i \neq j \neq n$), otherwise it is zero. Equation (26) states that all flows are non-negative.

The MIP model presented in Figure 1 assumes that the data and ACK transmission power levels are determined for each link considering the energy dissipations of node-i and node-j, only. Therefore, we should determine a single optimal power level for data packet transmission (l^{opt}_{ij}) and a single optimal power level for ACK packet transmission (k^{opt}_{ji}) for each link-

Maximize N_{rnd}

Subject to:

$$\sum_{(i,j)\in A} f_{ij} - \sum_{(j,i)\in A} f_{ji} = N_{rnd} s_i \ \forall i \in W \tag{20}$$

$$\sum_{(j,1)\in A} f_{j1} = N_{rnd} \sum_{j\in W} s_j \tag{21}$$

$$T_{bsy,i} = T_{slot} \left[\sum_{(i,j)\in A} \lambda_{ij}(l,k) f_{ij} + \sum_{(j,i)\in A} \lambda_{ji}(l,k) f_{ji} \right] + N_{rnd} T_{DA} \ \forall i \in W \tag{22}$$

$$\underbrace{\sum_{(i,j)\in A} E^D_{tx,ij}(l,k) f_{ij}}_{\textbf{transmission}} + \underbrace{P_{slp}(N_{rnd} T_{rnd} - T_{bsy,i})}_{\textbf{sleep}} + \underbrace{\sum_{(j,i)\in A} E^D_{rx,ji}(l,k) f_{ji}}_{\textbf{reception}} + \underbrace{N_{rnd} E_{DA}}_{\textbf{acquisiton}} \leq \varrho \ \forall i \in W \tag{23}$$

$$T_{slot} \left[\sum_{(i,j)\in A} \lambda_{ij}(l,k) f_{ij} + \sum_{(j,i)\in A} \lambda_{ji}(l,k) f_{ji} + \sum_{(j,n)\in A} \lambda_{jn}(l,k) f_{jn} I^i_{jn}(l,k) \right] \leq N_{rnd} T_{rnd}, \ \forall i \in V \tag{24}$$

$$I^i_{jn}(l,k) = \begin{cases} 1 \text{ if } P^{ant}_{rx,ji}(l) \geq P_{sns} \text{ or } P^{ant}_{rx,ni}(k) \geq P_{sns} \\ 0 \text{ o.w.} \end{cases} \tag{25}$$

$$f_{ij} \geq 0 \ \forall (i,j) \in A \tag{26}$$

Fig. 1: MIP framework.

(i, j) (*i.e.*, on link-(i, j) data packets are transmitted at power level-l^{opt}_{ij} by node-i and ACK packets are transmitted at power level-k^{opt}_{ji} by node-j). The power levels are determined by using the following link scope optimization scheme

$$\{l^{opt}_{ij}, k^{opt}_{ji}\} = \underset{l\in S_L k\in S_L}{\operatorname{argmin}} \left(E^D_{tx,ij}(l,k) + E^D_{rx,ji}(l,k) \right). \tag{19}$$

V. Analysis

In this section, we present the results of the numerical analysis to investigate the impact of path loss models on the WSN lifetime. We use a disk shaped network of radius R_{net} which consists of N_N sensor nodes randomly placed (uniform distribution) within the disk and a base station at the center. MATLAB is used to construct the data link layer (Section III-B) and General Algebraic Modeling System (GAMS) with CPLEX solver is used for the optimization problem (Section IV).

We consider a near-ground communication scenario (*i.e.*, a grassy park) where each node is deployed about 13 cm

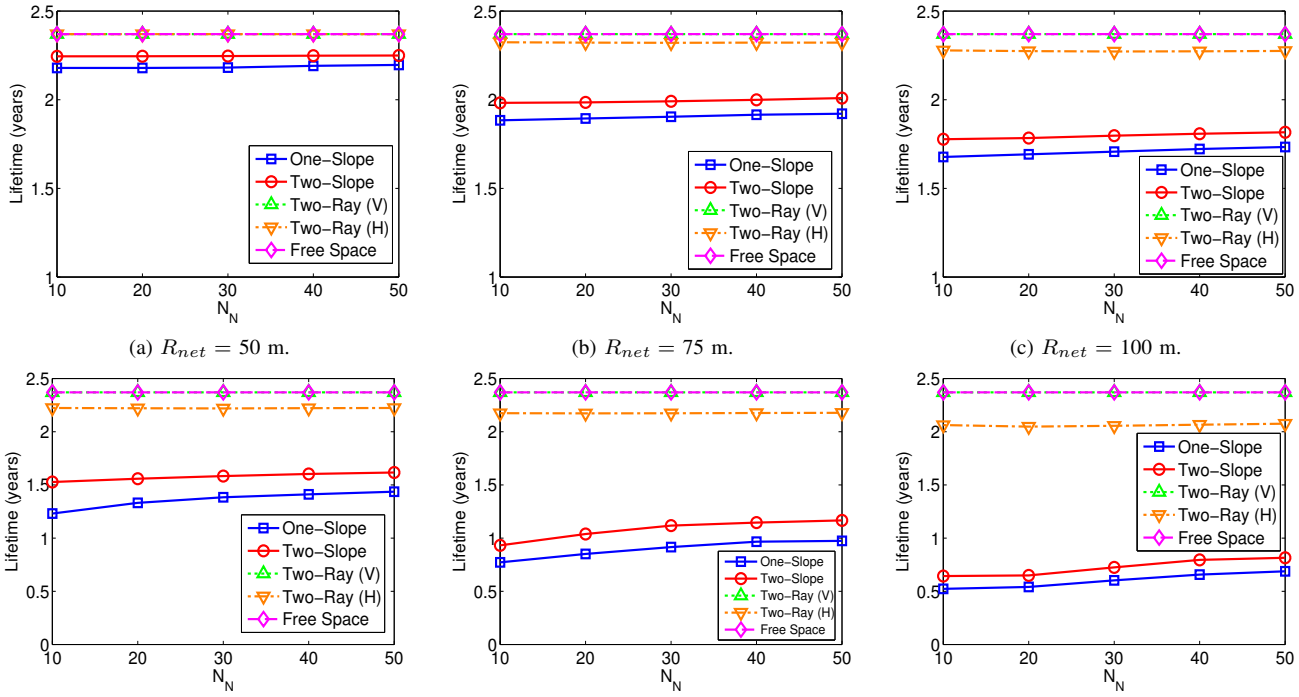

(a) $R_{net} = 50$ m. (b) $R_{net} = 75$ m. (c) $R_{net} = 100$ m.

(d) $R_{net} = 125$ m. (e) $R_{net} = 150$ m. (f) $R_{net} = 175$ m.

Fig. 2: Network lifetimes in terms of years as a function of N_N in the network for various R_{net} values.

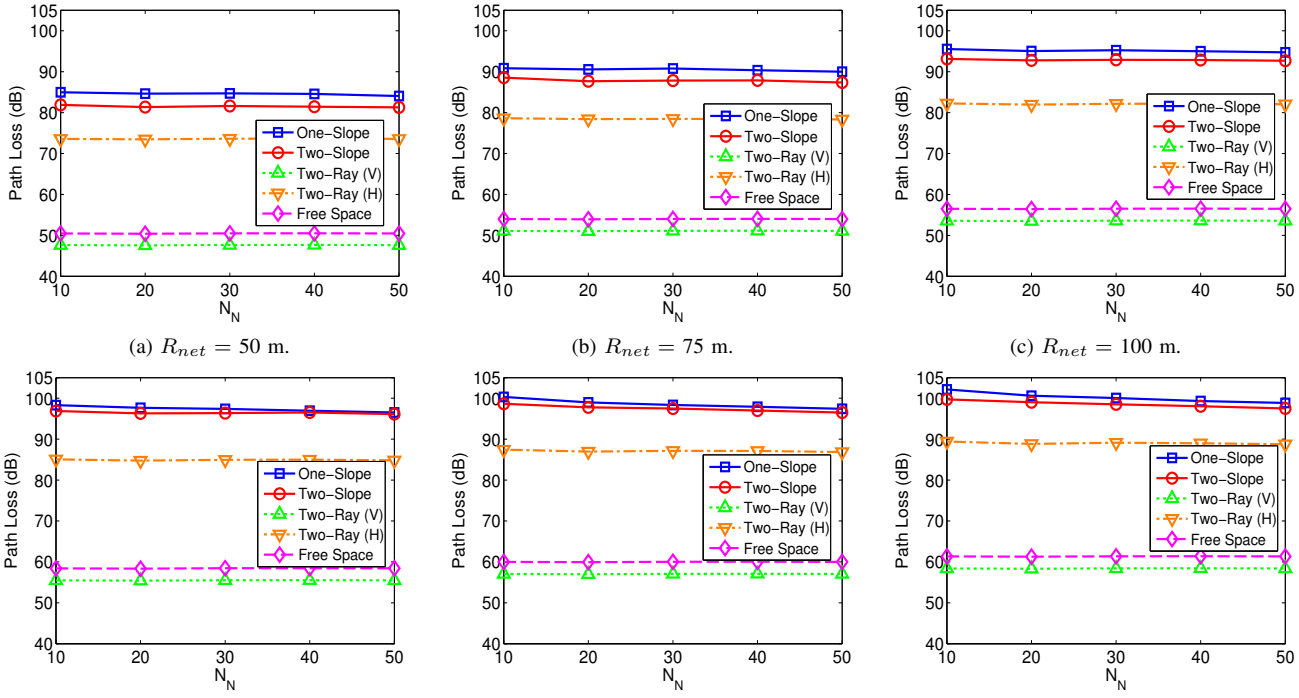

(a) $R_{net} = 50$ m. (b) $R_{net} = 75$ m. (c) $R_{net} = 100$ m.

(d) $R_{net} = 125$ m. (e) $R_{net} = 150$ m. (f) $R_{net} = 175$ m.

Fig. 3: Average path loss values (in dB) as a function of N_N in the network for various R_{net} values.

from the ground. For both one-slope and two-slope log-normal models, we use parameters values given in [4] which are empirically verified. The parameters for one-slope model are $PL(d_0) = 31$ dB, $n = 3.69$, and standard deviation of X_σ

is 1.42 dB, whereas the parameters of two-slope model are $PL(d_{01}) = 33$ dB, $PL(d_{02}) = 23$ dB, $n_1 = 2.09$, $n_2 = 4.01$, $d_b = 0.95$ m, and standard deviations of $X_{\sigma 1}$ and $X_{\sigma 2}$ are 0.28 dB and 0.67 dB, respectively. Since in this work CC1000 radios utilized with quarter wave monopole antennas, we take antenna gains as 5.19 dBi [13].

Standard deviations of the shadowing variables of two-slope model are much lower than the standard deviations of the single shadowing variable of one-slope model, therefore, two-slope model can represent the path loss characteristics of the measured data more accurately, hence, two-slope model is used as the reference model, in our analysis.

The results presented in Figure 2 and 3 are the averages of 100 independent runs (*i.e.*, 100 randomly generated topologies). The number of deployed nodes is varied from 10 to 50 nodes with six different network radii (*i.e.*, $R_{net} = 50$ m to 175 m). In Figure 2, all lifetime values are shown in terms of years for the given parameter set. Similarly in Figure 3, average path loss values for the utilized links (*i.e.*, links with non-zero flows) are presented in terms of dB.

Both the one-slope model and the two-slope model give the highest path loss values in all the cases we investigate in comparison to the path loss values obtained with all theoretical path loss models as anticipated because the theoretical models do not account for some of the dominant electromagnetic wave propagation mechanisms present in near-ground deployments. Two-ray model with horizontal polarization gives higher path loss values than the other theoretical models, yet, it's path loss values are still significantly lower than those of the empirical models. Nevertheless, network lifetimes obtained with theoretical models are much higher than the network lifetimes obtained with two-slope model. For example, lifetimes of free-space model, two-ray model with vertical polarization, and two-ray model with horizontal polarization are 191 %, 191 %, and 155 % higher than the lifetimes obtained with two-slope model for $R_{net} = 175$ m and $N_N = 50$.

For both two-ray model with vertical polarization and free-space model, network lifetime remain constant (2.37 years) regardless of the variations of R_{net} and N_N. Although the path loss values increase for all path loss models with increasing R_{net} due to the increasing transmitter receiver distance, path loss values obtained with two-ray model with vertical propagation and free-space model are so low that the minimum transmission power level suffices even for the largest R_{net} value (*i.e.*, all nodes can reach the base station directly by using the lowest transmission power level). We cannot increase R_{net} beyond 175 m because after this point network disconnections start to increase sharply (*e.g.*, with two-slope model more than 95 % of the randomly generated topologies are disconnected for $R_{net} = 250$ m).

Since one-slope model has one less degree of freedom in modeling the path loss, its path loss estimation accuracy is lower than two-slope model. Therefore, lifetimes obtained with one-slope model and two-slope model exhibit significant differences, especially for larger R_{net} values. For example, network lifetimes obtained with one-slope model is 4 % and 16 % lower than the lifetimes obtained with two-slope model for $R_{net} = 75$ m and $R_{net} = 150$ m, respectively ($N_N = 40$).

VI. Conclusion

We investigate the effects of path loss models on the WSN lifetime and build a detailed and accurate system model for energy dissipation by considering empirically verified characteristics of the Mica2 motes. We construct an MIP model to analyze the effects of path loss under idealized yet realistic settings. Our results reveal that adopting a theoretical model (free-space model and two-ray model) in analysis of near-ground WSNs can lead to more than 200 % lifetime estimation errors (*i.e.*, overestimation) when compared to two-slope model. The reason for such differences is that the evaluated theoretical models cannot capture the wave propagation mechanisms for near ground WSNs. Furthermore, one-slope model lifetime estimation errors also can be as high as 20 % (*i.e.*, underestimation) when compared to two-slope model. Nevertheless, the main conclusion of this study is that for correct assessment of the lifetimes of near-ground WSN deployments the use of pure theoretical models should, definitely, be avoided.

References

[1] M. Rahimi, R. Baer, O. Iroezi, J. Garcia, J. Warrior, D. Estrin, and M. Srivastava, "Cyclops: in situ image sensing and interpretation in wireless sensor networks," in *Proceedings of the ACM Conference on Embedded Networked Sensor Systems (SenSys)*, 2005, pp. 192–204.

[2] W. Heinzelman, A. Chandrakasan, and H. Balakrishnan, "An application specific protocol architecture for wireless microsensor networks," *IEEE Transactions on Wireless Communications*, vol. 1, pp. 660–670, 2002.

[3] Z. Cheng, M. Perillo, and W. Heinzelman, "General network lifetime and cost models for evaluating sensor network deployment strategies," *IEEE Transaction on Mobile Computing*, vol. 7, pp. 484–497, 2008.

[4] A. S. Martinez-Sala, J. M. M. G. Pardo, E. Egea-Lopez, J. Vales-Alonso, L. Juan-Llacer, and J. Garcia-Haro, "An accurate radio channel model for wireless sensor networks simulation." *Journal of Communications and Networks*, vol. 7, pp. 401–407.

[5] K. Sohrabi, B. Manriquez, and G. J. Potties, "Near-ground wideband channel measurements," in *Proceedings of the IEEE Vehicular Technology Conference (VTC)*, 1999, pp. 571–574.

[6] S. Kurt and B. Tavli, "Propagation model alternatives for outdoor wireless sensor networks," in *Proceedings of the IFIP Wireless Days (WD)*, 2013, pp. 1–3.

[7] T. S. Rappaport, *Wireless Communications: Principles and Practice*, 2nd ed. Piscataway, NJ, USA: Prentice Hall, 2002.

[8] H. Cotuk, B. Tavli, K. Bicakci, and M. B. Akgun, "The impact of bandwidth constraints on the energy consumption of wireless sensor networks," in *Proceedings of the IEEE Wireless Communication and Networking Conference (WCNC)*, 2014.

[9] A. Gogu, D. Nace, A. Dilo, and N. Meratnia, "Review of optimization problems in wireless sensor networks," in *Telecommunications Networks - Current Status and Future Trends*, J. Hamilton Ortiz, Ed. InTech, 2012, pp. 153–180.

[10] J. Vales-Alonso, E. Egea-Lopez, A. Martinez-Sala, P. Pavon-Marino, M. V. Bueno-Delgado, and J. Garcia-Haro, "Performance evaluation of MAC transmission power control in wireless sensor networks," *Computer Networks*, vol. 51, pp. 1483–1498, 2007.

[11] M. Zuniga and B. Krishnamachari, "Analyzing the transitional region in low power wireless links," in *Proceedings of the IEEE Communications Society Conference on Sensor, Mesh and Ad Hoc Communications and Networks (SECON)*, 2004, pp. 517–526.

[12] K. Bilinska, M. Filo, and R. Krystowski. (2007) Mica, Mica2, MicaZ. [Online]. Available: http://wwwpub.zih.tu-dresden.de/ dargie/wsn/slides/students/MICA.ppt

[13] T. Macnamara, *Introduction to Antenna Placement and Installation*, ser. Aerospace Series. Wiley, 2010.